Linear and Nonlinear Optical Response of Aromatic Amino Acids: A Time-Dependent Density Functional Investigation

J. Guthmuller* and D. Simon

Laboratoire de Spectrométrie ionique et moléculaire, Unité Mixte de Recherche 5579, Université Claude Bernard Lyon 1, and Centre National de la Recherche Scientifique, 43 Boulevard du 11 novembre 1918, F-69622 Villeurbanne Cedex, France

Received: May 18, 2006; In Final Form: June 22, 2006

The linear and nonlinear optical responses of the three aromatic amino acids tryptophan, tyrosine, and phenylalanine have been investigated by time-dependent density functional theory. The effect of the peptidic chain on the polarizabilities and the first hyperpolarizabilities is addressed by substituting different groups to the chromophores indole, phenol, and benzene. The optimized structures are in very good agreement with the experimental results. Furthermore, the calculated polarizabilities are found to match well with the empirical results, showing the evolution obtained as the chain is lengthened. A systematic and constant increase of the polarizability is found, for the three chromophores, for the various chain lengths. The first hyperpolarizability is also noticeably modified by the chains, but the evolution of this quantity is found to be more dependent on the system considered. Finally, it is suggested that each of the three aromatic amino acids has a significant contribution to the nonlinear response of proteins.

1. Introduction

The spectroscopic properties of the three aromatic amino acids, tryptophan (Trp), tyrosine (Tyr) and phenylalanine (Phe), have been largely used as a tool for the investigation of structure and chemical behavior of proteins.[1,2] From a crude structural point of view, tryptophan, tyrosine, and phenylalanine can be considered as monosubstituted indole, phenol, and benzene, respectively, the substitutent being in each case the amino acid group, $CH_2CH(NH_2)COOH$. The linear optical properties of the three amino acids are mainly determined by the chromophores indole, phenol, or benzene and are also strongly influenced by the local environment of the protein. Their spectral signatures allow the amino acids to be used as in situ structural probes for proteins in their background. For these reasons, and in order to understand and control there photophysical properties, a large number of experimental and theoretical studies have been performed on the chromophores indole,[3−8] phenol,[6,9] and benzene[6,9] and on the corresponding amino acids tryptophan,[10−17] tyrosine,[14,16,18,19] and phenylalanine.[14,18−22]

In addition, the nonlinear optical response of aromatic amino acids has been addressed more recently. Due to their π-conjugated electron density, which is polarizable and sensitive to the local environment of the protein, the three amino acids tryptophan, tyrosine, and phenylalanine might also be used as nonlinear probes. The nonlinear optical techniques appear to be a good way of providing structural and photophysical characteristics of interfacial systems[23,24] such as membrane proteins.[25] For example, second harmonic generation (SHG), the conversion of two photons of frequency ω into a single photon of frequency 2ω, is a nonlinear process allowed in noncentrosymmetric media only.[23,24] This technique has been applied in order to measure the hyperpolarizability of tryptophan residues that are surface-adsorbed at the air−water interface,[26−28] demonstrating the possibility of detecting proteins.

In the same way as for the linear spectroscopic properties, the development and understanding of the nonlinear response of suitable probes demand the common investigation at both experimental and theoretical levels. Concerning the theoretical studies, the determination of linear and nonlinear responses of molecules has been investigated in the literature by different approaches, going from semiempirical[29] to the most sophisticated ab initio[30,31] methods. Theoretical computations based on time-dependent density functional theory (TDDFT) have appeared in recent years to be very attractive since they allow rather fast calculations on large molecular systems.[32−34] For small molecules, it has been shown that the polarizabilities provided by the TDDFT are quite accurate.[35] Moreover, the application of TDDFT to the determination of the hyperpolarizabilities of metal pyridyl complexes,[36] metallabenzene-based chromophores,[37] and para-substituted nitrobenzenes and nitrostilbenes[33] match well with the experimental trends. Investigations on C_{60}[38] and on transition metal tetrapyrroles[39] have demonstrated the usefulness of theoretical calculations in order to clarify the experimental reported hyperpolarizabilities. However, the main cases in which TDDFT fails relate to the long π-conjugated chains,[40,41] for which both polarizabilities and hyperpolarizabilities are strongly overestimated. Fortunately, as discussed in a recent study,[31] this problem can be considered as largely solved if an appropriate exchange functional is used in the TDDFT processing.

The study presented here is a first-principles approach, based on DFT and TDDFT calculations. The three amino acids Trp, Tyr, and Phe are considered for the purpose of providing information concerning their possible use as nonlinear probes in a protein environment. To the best of our knowledge, no theoretical study on the nonlinear properties of Trp, Tyr, and Phe has been reported by now. In the first part we describe the structures of the different molecular systems investigated. The geometries of the chromophores indole, phenol, and benzene are reported and compared to experimental values. Then, in the second part, both the polarizabilities and hyperpolarizabilities

* Corresponding author. E-mail: jguth@lasim.univ-lyon1.fr.

10.1021/jp063053x CCC: $33.50
Published on Web 07/26/2006

of the different systems are considered and the effect of the peptidic chain on these properties is discussed.

2. Computational Method

The calculations have been carried out by use of the Amsterdam Density Functional (ADF) program.[42] The geometries have been optimized within the local density approximation treated in the Vosko−Wilk−Nusair[43] parametrization with nonlocal corrections to exchange due to Becke[44] and correlation due to Perdew[45] (BP). The molecular orbitals were expanded in a large basis set of Slater-type orbitals (TZ2P) taken from the ADF library. The TZ2P basis set is of double-ζ quality for the core electrons and of triple-ζ quality for the valence electrons. The basis set is augmented with polarization functions: 3d and 4f on C, N, and O and 2p and 3d on H.

The calculations of the linear and nonlinear optical responses have been determined with TDDFT as implemented in the ADF code.[46] The functional used for determining the response properties is the statistical average of orbital potential SAOP.[47] This functional has good asymptotic behavior in $-1/r$ for $r \rightarrow \infty$ and has been shown to be well-adapted, in comparison with LDA and GGA functionals, for the calculation of polarizabilities and hyperpolarizabilities of some small prototype molecules.[47,48] For example, the calculated hyperpolarizabilities[48] of NH_3, CO, H_2O, and HF are in good agreement with the CCSD(T) results of Sekino and Bartlett[49] and the value for CO is in rather good adequacy with the reference value reported by Maroulis.[50] Even if the transferability to larger molecules is not demonstrated, the SAOP potential is expected to provide a correct evolution of the response properties for the molecules considered here. For an accurate description of the response properties, which depend on the electronic density far from the nucleus, it is necessary to include diffuse functions to the basis set. Thereby, we used for the response calculations the recently developed ATZ2P[51] basis set, which is of comparable size to the TZ2P basis but augmented with diffuse functions: 3d, 4s, and 2p on C, N, and O and 2p and 1s on H. Larger basis sets, called QZ3P-1D and QZ3P-2D here (labeled ET-QZ3P-1DIFFUSE and ET-QZ3P-2DIFFUSE in the ADF library), have been also used in order to check the basis set convergence (section 4.1). These basis sets were developed and used in order to approximate the basis set limit for excitation energies and response properties.[48,51]

For the linear response, we report the average polarizability defined as

$$\langle\alpha\rangle = {}^1/_3(\alpha_{xx} + \alpha_{yy} + \alpha_{zz})$$

where the α_{ii} are the diagonal components of the polarizability, calculated in a molecular fixed coordinate system.

Only the second harmonic generation part of the nonlinear response has been considered. In this process, two photons of frequency ω are absorbed and simultaneously converted into a third photon of frequency 2ω. The hyperpolarizabilities are given in the B convention,[29] which is based on a perturbation series expansion of the induced dipole moment in terms of an external electric field. To compare our theoretical results we report the averaged quantities:

$$|\beta| = (\beta_x^2 + \beta_y^2 + \beta_z^2)^{1/2}$$

where

$$\beta_i = {}^1/_3 \sum_{j=x,y,z} (\beta_{ijj} + \beta_{jij} + \beta_{jji})$$

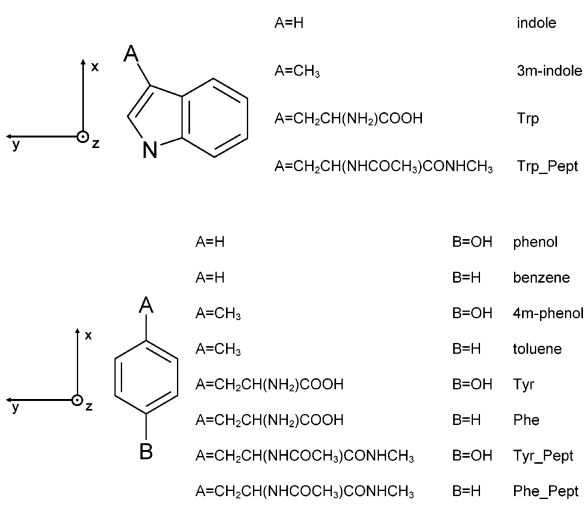

Figure 1. Axis systems, list, and nomenclature used for the various molecules considered.

for $i = x, y, z$ and

$$\beta_{\text{vec}} = \frac{\vec{\beta}.\vec{\mu}_0}{\mu_0}$$

where $\vec{\mu}_0$ and $\vec{\beta}$ are the permanent dipole moment of the molecule and the vector of components β_i, respectively. The projected hyperpolarizability β_{vec} corresponds to the quantity obtained from electric field-induced second harmonic generation (EFISH) measurements.

3. Structures

All the molecules are presented in Figure 1, together with the nomenclature used. The geometries have been optimized at the BP/TZ2P level of theory. First of all, the three aromatic chromophores indole, phenol, and benzene, corresponding to the side chains of the amino acids tryptophan, tyrosine, and phenylalanine, respectively, have been considered. Indole and phenol have been optimized in C_s symmetry while benzene belongs to the D_{6h} point group. In a second step, to take into account the effect of the peptidic chain, these chromophores were substituted by different groups. A methyl group (CH_3) has been added, leading to the systems 3m-indole, 4m-phenol, and toluene. Then, the three aromatic amino acids Trp, Tyr, and Phe have been considered. The optimized tryptophan corresponds to the most stable neutral conformer obtained from calculations of relative energies at the DFT and MP2 levels of theory, in agreement with experimental results.[11,12] This conformer is depicted in Figure 2. As has been pointed out by Snoek et al.,[12] the stability of this conformation can be explained by the presence of an intramolecular OH···NH_2 hydrogen bond, linking the carboxylic acid to the amino group. A distance of 1.824 Å has been obtained from the geometry optimization, which is a value in the typical scale of hydrogen bonds. Moreover, a hydrogen-bonded interaction between the hydrogen atom H_{11} (Figure 2) located on the amino group and the π-electron cloud of the aromatic ring may further increase its stability. The optimized conformation of Tyr and Phe is similar to the Trp conformer (see Figure 2). In the case of Phe, this conformer has been identified as the most stable by both DFT and MP2 calculations.[21] The same qualitative arguments than for Trp explain its stability. For example, the lengths of the intramolecular hydrogen bonds OH···NH_2 are similar to that for Trp: 1.826 and 1.836 Å for Tyr and Phe, respectively.

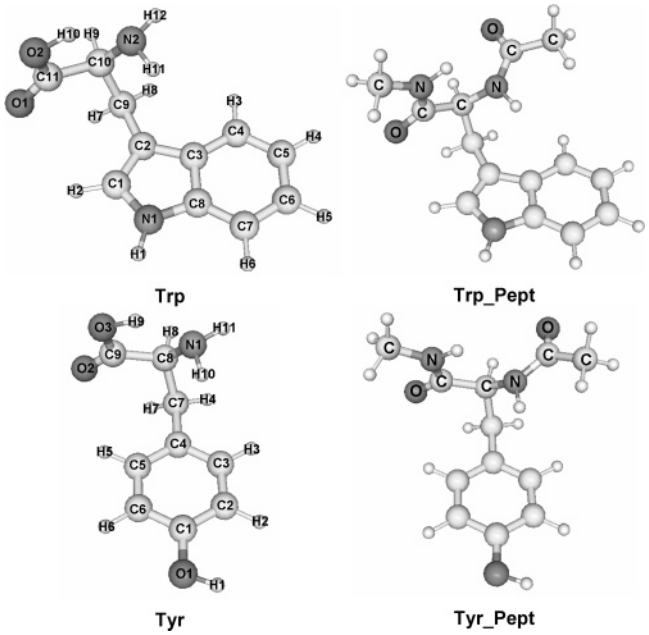

Figure 2. Conformation and atomic numbering of Trp, Trp_Pept, Tyr, and Tyr_Pept.

Finally, the systems with peptidic chain (Pept) were investigated (Figure 1). These structures are obtained from the corresponding amino acid conformers. The amino acid part is continued by two C−N peptidic bonds and the two nearest amino acids are described by methyl groups (CH_3). After geometry optimization, the conformation of the peptidic structures remains almost unchanged as compared to the amino acid conformers. For example, the torsion angles along the C−C bonds in the chain are modified by less than 10°.

To check the accuracy of the optimized structures, the calculated bond distances and angles of indole and phenol are reported in Table 1 and are compared to experimental data. The comparison is made with an experimental X-ray crystal structure of tryptophan[6] for indole and with a microwave measurement[52] for phenol. The mean deviations in the calculated bond lengths of indole and phenol with respect to the experimental values are 0.015 and 0.006 Å, respectively, while the corresponding mean deviations in the calculated bond angles are 2.4° and 0.2°, respectively. The agreement with the experimental structure of phenol is very good, whereas the errors for indole are larger. As it has been pointed out by Serrano-Andrés et al.,[3] the possible distortions and the artificial shortening of bonds resulting from the X-ray diffraction technique can explain the larger disagreement found for indole. This is particularly visible for the C1C2 and C3C8 bonds. The calculated bond distances for benzene, 1.398 Å for the C−C bond and 1.090 Å for the C−H bond, are in very good agreement with the experimental distances[6,9] 1.397 and 1.085 Å, respectively. The geometries obtained for 3m-indole, 4m-phenol, and toluene are very close to the corresponding chromophores indole, phenol, and benzene. The mean deviation of the bond distances between the theoretical structures is close to 0.002 Å for the three systems. Furthermore, the C−C bond linking the methyl group and the aromatic ring is found at 1.502, 1.512, and 1.511 Å for 3m-indole, 4m-phenol, and toluene, respectively. The value of 1.502 Å for 3m-indole is in very good agreement with the value of 1.500 Å calculated by Somers and Ceulemans[7] using the B3LYP functional. The geometrical parameters of Trp, Tyr, and Phe are not given in details. However, the mean deviations of the calculated bond distances with respect to the experimental diffraction values performed in HCl salt[13,18,22] are 0.032, 0.012, and 0.019 Å for Trp, Tyr, and Phe, respectively. It should be noted that, in this salt, the three amino acids are essentially present as positive ions. Therefore, in addition to the distortions due to the crystal structure, supplementary disagreements between theoretical and experimental values might result from the different charge distribution on the amino acid part. Finally, according to the experimental results, the errors in the bond lengths can be estimated to be less than 0.02 Å. Thereby, it can be concluded that the BP/TZ2P method gives a correct description of the structures investigated.

TABLE 1: Comparison between Calculated (BP/TZ2P) and Experimental Geometries for Indole and Phenol[a]

indole			phenol		
	calc	exp		calc	exp
N1C1	1.384	1.377	C1C2	1.401	1.391
C1C2	1.374	1.344	C2C3	1.397	1.394
C2C3	1.437	1.451	C3C4	1.397	1.395
C3C4	1.408	1.412	C4C5	1.399	1.395
C4C5	1.390	1.397	C5C6	1.394	1.392
C5C6	1.412	1.386	C6C1	1.400	1.391
C6C7	1.391	1.399	C2H2	1.093	1.086
C7C8	1.400	1.400	C3H3	1.090	1.084
C3C8	1.426	1.380	C4H4	1.089	1.080
C8N1	1.382	1.391	C5H5	1.090	1.084
N1C1C2	109.4	111.5	C6H6	1.089	1.081
C1C2C3	107.1	105.5	C1O1	1.377	1.375
C2C3C4	134.4	132.2	O1H1	0.971	0.957
C3C4C5	119.1	114.6	C1C2C3	119.7	119.4
C4C5C6	121.2	124.8	C2C3C4	120.5	120.5
C5C6C7	121.2	119.7	C3C4C5	119.3	119.2
C6C7C8	117.5	116.4	C4C5C6	120.8	120.8
			C5C6C1	119.5	119.2
			C6C1C2	120.1	120.9
			C1C2H2	119.9	120.0
			C2C3H3	119.3	119.5
			C3C4H4	120.3	120.3
			C4C5H5	120.0	119.8
			C5C6H6	121.5	121.6
			C2C1O1	122.5	122.1
			C6C1O1	117.4	117.0
			C1O1H1	108.5	108.8
Δd		0.015			0.006
$\Delta\varphi$		2.4			0.2

[a] The experimental results are taken from X-ray diffraction[6] and microwave[52] measurements. Δd and $\Delta\varphi$ refer to the absolute mean deviation error for bond length (in angstroms) and bond angles (in degrees).

4. Optical Response

4.1. Basis Set Effect. As has been pointed out above, the correct description of the response properties demands the inclusion of diffuse functions in the basis set. To check the accuracy of the basis, we report in Table 2 the mean polarizabilities $\langle\alpha\rangle$ and hyperpolarizabilities $|\beta|$ of indole, 3m-indole, and Trp calculated from different basis sets. The SHG hyperpolarizabilities have been determined for a wavelength of 1064 nm. The variations in percentage with respect to the QZ3P-2D basis are reported in parentheses; this basis is the larger one and is assumed to give the most accurate results. The errors due to the basis set for the mean static polarizabilities are comparable for the three molecules. TZ2P gives polarizabilities approximately 5% smaller than QZ3P-2D. The inclusion of diffuse functions in ATZ2P leads to errors less than 0.5%. Therefore, as can be seen from Table 2, the ATZ2P basis set gives polarizabilities close to the basis set convergence for the three systems considered. For the hyperpolarizabilities the inclusion of diffuse functions gives a more significant effect.

TABLE 2: Effect of the Basis Set on the Static Quantities $\langle\alpha\rangle$ and $|\beta|$ and on the SHG $|\beta|$ for Indole, 3m-Indole, and Trp[a]

molecule	property[b]	TZ2P	ATZ2P	QZ3P-1D	QZ3P-2D
indole	$\langle\alpha(0)\rangle$	99.38 (4.6)	104.10 (0.1)	103.59 (0.6)	104.18
	$\|\beta(0)\|$	0.655 (26.4)	0.511 (1.4)	0.550 (6.2)	0.518
	$\|\beta(-2\omega;\omega,\omega)\|$	0.828 (23.6)	0.666 (0.6)	0.710 (6.0)	0.670
3m-indole	$\langle\alpha(0)\rangle$	113.65 (3.9)	118.30 (0)	117.57 (0.6)	118.29
	$\|\beta(0)\|$	0.658 (10.5)	0.722 (1.8)	0.755 (2.7)	0.735
	$\|\beta(-2\omega;\omega,\omega)\|$	0.864 (12.0)	0.965 (1.7)	1.000 (1.8)	0.982
Trp	$\langle\alpha(0)\rangle$	150.15 (4.1)	155.87 (0.4)	155.40 (0.7)	156.52
	$\|\beta(0)\|$	1.481 (9.7)	1.288 (4.6)	1.281 (5.1)	1.350
	$\|\beta(-2\omega;\omega,\omega)\|$	1.885 (10.6)	1.608 (5.6)	1.599 (6.2)	1.704

[a] The hyperpolarizabilities are given in the B convention. The variations in percentage in respect to the QZ3P-2D basis are reported in parentheses. [b] $\langle\alpha\rangle$, atomic units; $|\beta|$, 10^{-30} esu; $|\beta|$, SHG calculated at 1064 nm.

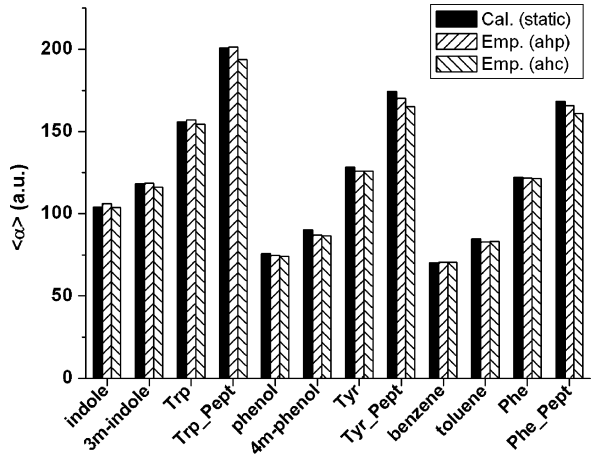

Figure 3. Static average polarizability (atomic units) for the various molecules. (ahp) and (ahc) correspond to empirical values.

For TZ2P the errors reach almost 30% for indole and nearly 10% for 3m-indole and Trp. The errors are again significantly reduced for the ATZ2P basis, with values close to 1%, 2%, and 5% for indole, 3m-indole, and Trp, respectively. The results obtained with this basis set are even closer to the values calculated with QZ3P-2D than the hyperpolarizabilities determined with the QZ3P-1D basis. As a consequence, the ATZ2P basis appears to be well-adapted for an accurate determination of polarizabilities and hyperpolarizabilities with a reasonable computational cost. The errors are estimated to be close to 5% from the basis set limit for the molecules considered. Hence, this basis set was used, in the following, to determine the optical responses of all systems studied.

4.2. Polarizabilities. In this part, the linear optical response of the different molecules investigated is described. An accurate estimation of the linear response seems to be a necessary condition before the nonlinear response is examined. The mean static polarizabilities are reported in Figure 3 for all the systems considered. The theoretical polarizabilities are compared to empirical values estimated by additivity methods.[53] These values are obtained by use of two different empirical formulas, one based on atomic hybrid polarizabilities (ahp) and the other on atomic hybrid components (ahc). According to the results of Miller,[53] the empirical values reproduce the experimental polarizabilities to an average error of approximately 3% for the type of compounds considered in this work. For example, the experimental values of benzene and toluene, 70.3 and 82.7 au,[53] respectively, are in very good agreement with the empirical results obtained through the (ahp) formula, 70.4 and 82.8 au, respectively, and the (ahc) formula, 70.5 and 82.9 au, respectively. Therefore, the (ahp) and (ahc) empirical polarizabilities appear to be well-adapted to check the accuracy of the theoretical results. In Figure 3, it can be seen that the calculated polarizabilities are in very good agreement with the empirical values. The mean deviation between the theoretical values and the polarizabilities obtained with the (ahp) and (ahc) methods are 1.7 and 3.3 au, respectively. This corresponds to an average error of 1.4% and 2.3% for (ahp) and (ahc), respectively, when compared with the calculated polarizabilities. As a consequence, it can be concluded that the calculated polarizabilities are accurately determined and that the evolution between the different systems is well reproduced. For each chromophore, the polarizability is significantly increased when the aromatic rings are substituted by the various chains. For example, the polarizability is increased by 14%, 50%, and 93% when the indole ring is substituted to give 3m-indole, Trp, and Trp_Pept, respectively. Moreover, similar increases are obtained for a given chain. The variations are 14.2, 14.6, and 14.6 au for 3m-indole, 4m-phenol, and toluene, respectively; 51.8, 52.6, and 52.2 au for Trp, Tyr, and Phe, respectively; and 96.9, 98.6, and 98.3 au for Trp_Pept, Tyr_Pept, and Phe_Pept, respectively. The close values obtained for these increases suggest that the evolution of the polarizabilities is mainly due to the polarizability of the various chains. This is also indicated by the validity of additivity methods for evaluating molecular polarizabilities. Furthermore, the correct evolution obtained for the different systems and the agreement between calculated and empirical polarizabilities show that the systems considered here do not present the problematic overestimation of $\langle\alpha\rangle$. Such a behavior, when the chain length increases, has been encountered, for example, for polyacetylene chains and push−pull π-conjugated systems.[40,41] The good results obtained for the polarizability suggest that the employed method can also yield a correct description of the nonlinear response.

4.3. Hyperpolarizabilities. In the static case, the hyperpolarizability tensor β is symmetric in all permutations of the Cartesian indices (Kleinman symmetry[54]), which reduces the number of components to 10. The hyperpolarizabilities components and the hyperpolarizabilities $|\beta|$ and β_{vec}, given in the B convention, for the various systems considered, are reported in Tables 3 and 4. The coordinate systems used for the molecules in connection with Trp and for the molecules in connection with Tyr and Phe are depicted in Figure 1. For each system, the *x* and *y* axes are in the plane of the aromatic rings. For the indole rings, the *x* axis is along the C8C3 bond, while the *y* axis passes through the C1 carbon atom. On the other hand, for the benzene and phenol rings, the *x* axis passes through the carbon atoms C1 and C4, while the *y* axis passes through the C6 atom.

Let us start by considering the hyperpolarizability of the aromatic side chains. Due to its center of inversion, the first hyperpolarizability of benzene is equal to zero. The β tensor of indole is dominated by the diagonal component β_{yyy} with a value of 0.45×10^{-30} esu, whereas the main component for phenol

TABLE 3: Static First Hyperpolarizabilities Components, $|\beta|$ and β_{vec} (10^{-30} esu) for the Systems in Connection with Trp[a]

components	indole	3m-indole	Trp	Trp_Pept
XXX	−0.08	−0.18	−0.54	−0.16
YYY	0.45	0.69	1.06	1.15
ZZZ	0.00	−0.02	−0.06	−0.23
XYY	0.02	0.08	−0.05	0.11
XZZ	−0.09	−0.07	−0.19	−0.28
YXX	0.04	−0.05	−0.16	0.31
YZZ	0.00	0.06	0.09	0.20
ZXX	0.00	−0.03	−0.14	−0.34
ZYY	0.00	0.03	−0.09	−0.19
XYZ	0.00	−0.02	−0.11	0.14
$\|\beta\|$	0.51	0.72	1.29	1.86
β_{vec}	0.45	0.65	−0.89	−0.61

[a] Given in the B convention.

is β_{xxx} with a value of -0.83×10^{-30} esu. These components dominate in the average hyperpolarizability $|\beta|$ with values of 0.51×10^{-30} and 0.96×10^{-30} esu for indole and phenol, respectively. For indole, the projected hyperpolarizability β_{vec} is obtained with a value of 0.45×10^{-30} esu comparable to that of $|\beta|$, whereas for phenol β_{vec} is found at -0.27×10^{-30} esu. The absolute value of β_{vec} for phenol is in global agreement with the experimental EFISH result measured by Oudar et al.[55] at 0.17×10^{-30} esu. The difference in sign can be explained[56] by the inaccurate direction of the dipole moment taken by Oudar et al. Thus, the hyperpolarizability tensors of indole and phenol show a simple structure with one diagonal component giving the main contribution to β.

Next, we investigate the effect of the different chains and in what way the hyperpolarizability tensor is modified. Let us first describe the evolution of the components for the different molecules in connection with Trp. From Table 3, it can be seen that the diagonal component β_{yyy} dominates the nonlinear response of indole, 3m-indole, Trp, and Trp_Pept with values of 0.45×10^{-30}, 0.69×10^{-30}, 1.06×10^{-30}, and 1.15×10^{-30} esu, respectively. In the case of Trp the component β_{xxx} gives also a significant contribution to the β tensor with a value of -0.54×10^{-30} esu, whereas for Trp_Pept many nondiagonal components have significant contributions with absolute values around 0.3×10^{-30} esu. The average hyperpolarizability $|\beta|$ with values of 0.51×10^{-30}, 0.72×10^{-30}, 1.29×10^{-30}, and 1.86×10^{-30} esu for indole, 3m-indole, Trp, and Trp_Pept, respectively, is correlated to the large increase found for the diagonal component β_{yyy}. This leads to a value of $|\beta|$ for Trp_Pept, approximately 3.6 times higher than for indole. The behavior of the projected hyperpolarizability β_{vec} is different. Similar to $|\beta|$, it is increased when going from indole to 3m-indole. However, the sign is reversed and a decrease is found for the absolute value between Trp and Trp_Pept. The change in sign is related to the modified direction of the dipole moment due to the additional contribution of the amino acid and peptidic chains.

Let us describe the hyperpolarizabilities corresponding to the systems in connection with Tyr and Phe. These hyperpolarizabilities are reported in Table 4. For phenol, 4m-phenol, and Tyr, the diagonal component β_{xxx} gives the main contribution to the β tensor with values of -0.83×10^{-30}, -0.90×10^{-30}, and -1.16×10^{-30} esu, respectively, whereas it is not the main component for Tyr_Pept, since its absolute value is decreased to 0.17×10^{-30} esu. Moreover, the diagonal component β_{yyy} gives a significant contribution to Tyr and to Tyr_Pept with values of 0.45×10^{-30} and 0.44×10^{-30} esu, respectively. The β tensor of Tyr_Pept is found with a complex structure in which both diagonal and nondiagonal components give a similar contribution. In the same way as for Trp, $|\beta|$ is increased when going from phenol to 4m-phenol and Tyr. However, $|\beta|$ is obtained with a lower value for Tyr_Pept in comparison with Tyr, 1.18×10^{-30} and 1.51×10^{-30} esu, respectively. β_{vec} is found to be negative and its absolute values follow a similar evolution to $|\beta|$. The complicated hyperpolarizability tensor and the resulting decrease found for Tyr_Pept shows the neat effect of the peptidic chain, modifying significantly the β components of phenol. This is illustrated by the clear reduction of the β_{xxx} component when going from phenol to Tyr_Pept.

Last, the molecules in connection with Phe are described. The diagonal component β_{xxx} dominates the β tensor of toluene and Phe_Pept with values of 0.18×10^{-30} and 0.97×10^{-30} esu, respectively, whereas for Phe the main component is β_{yyy} and is found at 0.40×10^{-30} esu. β_{xxx} gives also a significant contribution to Phe with a value of 0.20×10^{-30} esu and β_{yyy} to Phe_Pept with a value of 0.43×10^{-30} esu. Again, some nondiagonal components take part to the β tensor of the molecule with peptidic chain Phe_Pept, with values of -0.43×10^{-30} and 0.25×10^{-30} esu for β_{zyy} and β_{yzz}, respectively. Additionally, it can be seen that the evolution of the main components, from Tyr to Tyr_Pept and from Phe to Phe_Pept, is comparable. For example, the diagonal component β_{xxx} increases significantly from Tyr to Tyr_Pept and from Phe to Phe_Pept, inferring a positive contribution of the peptidic chain. Furthermore, β_{yyy} is almost unchanged for these systems with values close to 0.40×10^{-30} esu and the nondiagonal components β_{zyy} and β_{yzz} follow a similar behavior with values of -0.43×10^{-30} esu and close to 0.30×10^{-30} esu, respectively, for the systems with peptidic chains. The evolution of $|\beta|$ for the systems in connection with Phe is comparable to the behavior obtained for the systems in connection with Trp. A strong increase is found for $|\beta|$ when going from toluene to Phe_Pept with values of 0.19×10^{-30} and 1.35×10^{-30} esu, respectively. The sign of β_{vec} is also reversed between toluene and Phe. However, the absolute value of β_{vec} is further increased for Phe_Pept.

Similarly to the behavior of the polarizabilities, the chains have a large effect on the hyperpolarizability tensor. For both quantities, an increase is found when the aromatic side chains are substituted. However, in contrast with $\langle\alpha\rangle$, for which a regular increase has been found between the various systems, the hyperpolarizability tensor and the related quantities $|\beta|$ and β_{vec} show a more complex behavior. For example, the evolution of $|\beta|$ is depicted in Figure 4. In the same way as for $\langle\alpha\rangle$, a strong increase, as the chain length becomes longer, has been found for the systems in connection with Trp and Phe, whereas the hyperpolarizability $|\beta|$ obtained is lower for Typ_Pept in comparison to Tyr. This different evolution might be due to the particular interaction occurring between the different aromatic chromophores and the associated chains. In particular, the decrease found between Tyr and Tyr_Pept can be related to the increase obtained for the negative diagonal component β_{xxx} due to the peptidic chain. It shows that the various chains contribute significantly to the hyperpolarizability and that a description limited to the aromatic rings appears to be insufficient. Moreover, the three amino acids investigated are found with a hyperpolarizability of a comparable magnitude. Thus, they are all expected to give a significant contribution to the nonlinear response of a given protein.

Finally, the effect of frequency dispersion is addressed. In Figure 4, the dynamic hyperpolarizabilities $|\beta(-2\omega; \omega, \omega)|$, corresponding to the second harmonic generation calculated at

TABLE 4: Static First Hyperpolarizabilities Components, $|\beta|$ and β_{vec} (10^{-30} esu) for the Systems in Connection with Tyr and Phe[a]

components	phenol	4*m*-phenol	Tyr	Tyr_Pept	toluene	Phe	Phe_Pept
XXX	−0.83	−0.90	−1.16	−0.17	0.18	0.20	0.97
YYY	0.06	0.09	0.45	0.44	0.02	0.40	0.43
ZZZ	0.00	−0.02	−0.06	−0.20	−0.03	−0.03	−0.11
XYY	0.02	0.02	0.09	−0.01	−0.02	0.05	−0.10
XZZ	−0.14	−0.11	−0.17	−0.06	0.04	−0.01	0.14
YXX	0.07	0.07	0.22	0.19	0.00	0.16	0.09
YZZ	0.01	−0.01	0.13	0.33	−0.02	0.12	0.25
ZXX	0.00	−0.01	−0.14	−0.02	0.00	−0.02	0.10
ZYY	0.00	0.02	−0.06	−0.43	0.02	−0.07	−0.43
XYZ	0.00	0.00	0.00	0.10	0.00	0.00	0.07
$\|\beta\|$	0.96	0.99	1.51	1.18	0.19	0.73	1.35
β_{vec}	−0.27	−0.52	−0.67	−0.52	0.19	−0.71	−1.24

[a] Given in the B convention.

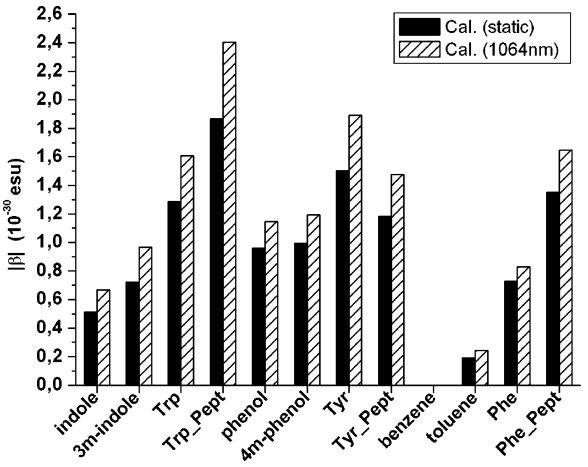

Figure 4. Static and dynamic (at 1064 nm) hyperpolarizabilities $|\beta|$ (10^{-30} esu) for the various systems, given in the B convention.

a wavelength of 1064 nm, are depicted. At this frequency the hyperpolarizabilities are still in the off-resonant region. The nearest resonances for Trp, Tyr, and Phe are obtained for wavelengths close to 570,[10,28] 560,[19] and 530 nm,[19] respectively. The frequency-dependent hyperpolarizability follows an evolution similar to that of the static $|\beta|$. The effect of dispersion at 1064 nm is to increase the hyperpolarizability $|\beta|$ by approximately 25% for the various molecules. For example, the increase due to dispersion is 29%, 25%, and 22% for Trp_Pept, Tyr_Pept, and Phe_Pept, respectively. Comparable variations are found for each component of the β tensor. The effect of frequency dispersion appears to be significant even in the off-resonant region. Thereby, it is necessary to include this effect in order to obtain accurate hyperpolarizabilities.

5. Conclusions

We have investigated, by using a TDDFT method, the linear and nonlinear optical response of the three aromatic chromophores indole, phenol, and benzene. The evaluation of the effect of various chains on the optical response has been done by substituting the chromophores by a methyl group, an amino acid part, and a chain possessing two peptidic bonds. The geometries optimized by DFT are in good agreement with the experimental structures. The effect of the basis set on the optical response has been investigated, and the need to include diffuse functions has been shown. The use of the recently developed ATZ2P basis set has shown to yield polarizabilities and hyperpolarizabilities at approximately 0.5% and 5% from the basis set limit, respectively. The calculated polarizabilities are in very good agreement with the empirical values, illustrating the accuracy of the method. The various chains have a strong effect on both polarizabilities and hyperpolarizabilities. The different chains lead to a systematic and almost constant increase of the polarizability, which can be related to the polarizability of the chains. The effect of the chains on the hyperpolarizability is more complex. The evolution of the various β components has been described in detail for the different molecules considered. It appears that the effect is less systematic and depends on the component and the quantity considered. For example, as can be seen from Figure 4, the average hyperpolarizability $|\beta|$ is in most cases increased when the chain is lengthened. The particular decrease obtained for Tyr_Pept can be related to the increase, found for both Tyr_Pept and Phe_Pept, of the β_{xxx} component.

Finally, our study leads to the following conclusions. The three aromatic amino acids considered show hyperpolarizability tensors of comparable intensity. They are then expected to contribute, in an equivalent way, to the nonlinear response in protein. Additionally, it appears that a correct description of the peptidic chain is required in order to model the nonlinear response of chromophores in protein. The variations of the hyperpolarizabilities due to the additional chains are of the same order of magnitude as the hyperpolarizabilities of the corresponding chromophores. This shows that, at least in the off-resonant case, the optical nonlinear properties of the protein cannot be restricted to the response of the chromophores' aromatic rings.

Acknowledgment. This work was supported by the French Research Ministry and the Centre National de la Recherche Scientifique (CNRS) under Contract AC/DRAB03/15. We thank the Centre Informatique National de l'Enseignement Supérieur (CINES) at Montpellier (France) for generous allocation of computation time under Contract c20050822452.

References and Notes

(1) Lakowicz, J. R. *Principles of Fluorescence Spectroscopy*; Kluwer Academic/Plemum Publishers: New York, 1999.
(2) Callis, P. R. *Methods Enzymol.* **1997**, *278*, 113.
(3) Serrano-Andrés, L.; Roos, B. O. *J. Am. Chem. Soc.* **1996**, *118*, 185.
(4) Serrano-Andrés, L.; Borin, A. C. *Chem. Phys.* **2000**, *262*, 267.
(5) Borin, A. C.; Serrano-Andrés, L. *Chem. Phys.* **2000**, *262*, 253.
(6) Rogers, D. M.; Hirst, J. D. *J. Phys. Chem. A* **2003**, *107*, 11191.
(7) Somers, K. R. F.; Ceulemans, A. *J. Phys. Chem. A* **2004**, *108*, 7577.
(8) Dedonder-Lardeux, C.; Jouvet, C.; Perun, S.; Sobolewski, A. L. *Phys. Chem. Chem. Phys.* **2003**, *5*, 5118.
(9) Lorentzon, J.; Malmqvist, P.; Fülscher, M.; Roos, B. O. *Theor. Chim. Acta* **1995**, *91*, 91.
(10) Rizzo, T. R.; Park, Y. D.; Peteanu, L. A.; Levy, D. H. *J. Chem. Phys.* **1986**, *84*, 2534.

(11) Compagnon, I.; Hagemeister, F. C.; Antoine, R.; Rayane, D.; Broyer, M.; Dugourd, P.; Hudgins, R. R.; Jarrold, M. F. *J. Am. Chem. Soc.* **2001**, *123*, 8440.
(12) Snoek, L. C.; Kroemer, R. T.; Hockridge, M. R.; Simons, J. P. *Phys. Chem. Chem. Phys.* **2001**, *3*, 1819.
(13) Cao, X.; Fischer, G. *J. Phys. Chem. A* **1999**, *103*, 9995.
(14) Kushwaha, P. S.; Mishra, P. C. *J. Photochem. Photobiol. A* **2000**, *137*, 79.
(15) Rogers, D. M.; Besley, N. A.; Shea, P. O.; Hirst, J. D. *J. Phys. Chem. B* **2005**, *109*, 23061.
(16) Tong, J.; Li, X. Y. *Chem. Phys.* **2002**, *284*, 543.
(17) Nolting, D.; Marian, C.; Weinkauf, R. *Phys. Chem. Chem. Phys.* **2004**, *6*, 2633.
(18) Hameka, H. F.; Jensen, J. O. *J. Mol. Struct.* **1993**, *288*, 9.
(19) Martinez, S. J.; Alphano, J. C.; Levy, D. H. *J. Mol. Spectrosc.* **1992**, *156*, 421.
(20) Lee, K. T.; Sung, J.; Lee, K. J.; Kim, S. K.; Park, Y. D. *Chem. Phys. Lett.* **2003**, *368*, 262.
(21) Snoek, L. C.; Robertson, E. G.; Kroemer, R. T.; Simons, J. P. *Chem. Phys. Lett.* **2000**, *321*, 49.
(22) Cao, X.; Fischer, G. *J. Mol. Struct.* **2000**, *519*, 153.
(23) Corn, R. M.; Higgins, D. A. *Chem. Rev.* **1994**, *94*, 107.
(24) Eisenthal, K. B. *Chem. Rev.* **1996**, *96*, 1343.
(25) Rinuy, J.; Brevet, P. F.; Girault, H. H. *Biophys. J.* **1999**, *77*, 3350.
(26) Crawford, M. J.; Haslam, S.; Probert, J. M.; Gruzdkov, Y. A.; Frey, J. G. *Chem. Phys. Lett.* **1994**, *229*, 260.
(27) Smiley, B. L.; Vogel, V. *J. Chem. Phys.* **1995**, *103*, 3140.
(28) Mitchell, S. A.; McAloney, R. A. *J. Phys. Chem. B* **2004**, *108*, 1020; corrected in *J. Phys. Chem. B* **2005**, *109*, 15178.
(29) Willetts, A.; Rice, J. E.; Burland, D. M.; Shelton, D. P. *J. Chem. Phys.* **1992**, *97*, 7590.
(30) Sałek, P.; Helgaker, T.; Vahtras, O.; Ågren, H.; Jonsson, D.; Gauss, J. *Mol. Phys.* **2005**, *103*, 439.
(31) Bulat, F. A.; Toro-Labbé, A.; Champagne, B.; Kirtman, B.; Yang, W. *J. Chem. Phys.* **2005**, *123*, 014319.
(32) van Gisbergen, S. J. A.; Snijders, J. G.; Baerends, E. J. *J. Chem. Phys.* **1998**, *109*, 10644.
(33) Heinze, H. H.; Della Sala, F.; Görling, A. *J. Chem. Phys.* **2002**, *116*, 9624.
(34) Sałek, P.; Vahtras, O.; Helgaker, T.; Ågren, H. *J. Chem. Phys.* **2002**, *117*, 9630.
(35) van Gisbergen, S. J. A.; Osinga, V. P.; Gritsenko, O. V.; van Leeuwen, R.; Snijders, J. G.; Baerends, E. J. *J. Chem. Phys.* **1996**, *105*, 3142.
(36) Coe, B. J.; Jones, L. A.; Harris, J. A.; Brunschwig, B. S.; Asselberghs, I.; Clays, K.; Persoons, A.; Garín, J.; Orduna, J. *J. Am. Chem. Soc.* **2004**, *126*, 3880.
(37) Karton, A.; Iron, M. A.; van der Boom, M. E.; Martin, J. M. L. *J. Phys. Chem. A* **2005**, *109*, 5454.
(38) van Gisbergen, S. J. A.; Snijders, J. G.; Baerends, E. J. *Phys. Rev. Lett.* **1997**, *78*, 3097.
(39) Ricciardi, G.; Rosa, A.; van Gisbergen, S. J. A.; Baerends, E. J. *J. Phys. Chem. A* **2000**, *104*, 635.
(40) Champagne, B.; Perpète, E. A.; van Gisbergen, S. J. A.; Baerends, E. J.; Snijders, J. G.; Soubra-Ghaoui, C.; Robins, K. A.; Kirtman, B. *J. Chem. Phys.* **1998**, *109*, 10489.
(41) Champagne, B.; Perpète, E. A.; Jacquemin, D.; van Gisbergen, S. J. A.; Baerends, E. J.; Soubra-Ghaoui, C.; Robins, K. A.; Kirtman, B. *J. Phys. Chem. A* **2000**, *104*, 4755.
(42) Te Velde, G.; Bickelhaupt, F. M.; Baerends, E. J.; Fonseca Guerra, C.; van Gisbergen, S. J. A.; Snijders, J. G.; Ziegler, T. *J. Comput. Chem.* **2001**, *22*, 931.
(43) Vosko, S. H.; Wilk, L.; Nusair, M. *Can. J. Phys.* **1980**, *58*, 1200.
(44) Becke, A. D. *Phys. Rev. A* **1988**, *38*, 3098.
(45) Perdew, J. P. *Phys. Rev. B* **1986**, *33*, 8822.
(46) van Gisbergen, S. J. A.; Snijders, J. G.; Baerends, E. J. *Comput. Phys. Commun.* **1999**, *118*, 119.
(47) Schipper, P. R. T.; Gritsenko, O. V.; van Gisbergen, S. J. A.; Baerends, E. J. *J. Chem. Phys.* **2000**, *112*, 1344.
(48) Grüning, M.; Gritsenko, O. V.; van Gisbergen, S. J. A.; Baerends, E. J. *J. Chem. Phys.* **2002**, *116*, 9591.
(49) Sekino, H.; Bartlett, R. J. *J. Chem. Phys.* **1993**, *98*, 3022.
(50) Maroulis, G. *J. Phys. Chem.* **1996**, *100*, 13466.
(51) Chong, D. P. *Mol. Phys.* **2005**, *103*, 749.
(52) Larsen, N. W. *J. Mol. Struct.* **1979**, *51*, 175.
(53) Miller, K. J. *J. Am. Chem. Soc.* **1990**, *112*, 8533.
(54) Kleinman, D. A. *Phys. Rev.* **1962**, *126*, 1977.
(55) Oudar, J. L.; Chemla, D. S.; Batifol, E. *J. Chem. Phys.* **1977**, *67*, 1626.
(56) Guthmuller, J.; Simon, D. *J. Chem. Phys.* **2006**, *124*, 174502.